ACTA STEREOL 1990; 9/1: 37-52
PROC ECS 5 FREIBURG I. BR. 1989
REVIEW ARTICLE

FRACTAL MODELS IN BIOLOGICAL IMAGE ANALYSIS AND VISION +

Jean Paul Rigaut

Laboratoire de Microscopie Quantitative en Histopathologie,
U.263 INSERM, Université Paris 7,
Tour 53-1, 2 place Jussieu, 75251 - Paris Cédex 05, France

ABSTRACT

The mathematical bases and the main features of classic and asymptotic fractal formalisms are explained, together with a review of methods for the estimation of the fractal dimension and of other quantities.

The main applications of fractal geometry in the analysis of images from cell and tissue biology are reviewed.

Finally, the relationships between mathematical morphology and fractal geometry are explored, starting from a new equation which links the two theories. This represents a basis for low resolution segmentation and texture recognition in artificial vision. Possible relationships with human vision are discussed.

Keywords: Fractal geometry, mathematical morphology, image analysis, vision, biology.

INTRODUCTION

Fractal geometry allows an objective description of many types of hitherto mathematically undescribable natural objects (e.g. Mandelbrot, 1982; Rigaut, 1984, 1987b; Feder, 1988; Peitgen & Saupe, 1988).

Fractal theory represents also a basis for the creation of synthetic images of all sorts (e.g. Mandelbrot, 1982; Barnsley, 1988; Peitgen & Saupe, 1988).

Finally, since their recent marriage with chaos theories (e.g. Barnsley, 1988; Peitgen & Saupe, 1988) fractals can often be considered as attractors in a dynamical system. Synthetic images which imitate complex natural scenes can be obtained as fractal attractors of a recurrent procedure (Barnsley, 1988). The formalism of neurocomputers (e.g. Kohonen, 1988), which offers an attractive basis for artificial and human vision, includes a chaos/attractor paradigm.

A short review of applications of fractal geometry to cell and tissue biology will be offered. The reader is referred to Rigaut (1987b) for applications to other aspects of biology. Simple mathematical bases will be given (for more rigorous treatments, cf. e.g. Mandelbrot, 1982; Falconer, 1985; Barnsley, 1988; Feder, 1988; Rigaut, 1990).

+ Keynote lecture presented at ECS 5, Freiburg.

FRACTAL GEOMETRY IN CYTOLOGY AND HISTOLOGY

The classic fractal concept

An empirical equation represents the basis of the concept. Richardson (1961) discovered that coastline lengths (B) produce linear log-log graphs, with a negative slope, when plotted versus the length (η) of a yardstick representing an inverse measure of the resolution. Mandelbrot's (1967) interpretation of Richardson's empirical relationship forms the basis of fractal geometry. Let B_η be the coastline's length at resolution η^{-1}, and β and D be positive constants. The empirical Richardson-Mandelbrot equation is then

$$B_\eta \sim \beta \, \eta^{1-D} \quad . \qquad (1)$$

Let the yardstick be a divider, stepping along the coastline with different step-lengths (η) and let N_η be the number of steps covering the coastline. As $B_\eta = N_\eta \, \eta$, $\beta \sim N_\eta \, \eta^D$. Therefore, β is a length when D=1. When $D \in (1, 2)$, β can be understood as being a constant measure of B_η in dimension D (Mandelbrot, 1967). The coastline is then fractal, with fractal dimension D (Mandelbrot, 1982). The coastline is smooth if D=1; its apparent roughness increases with D.

In a more general way, if D_T is the topological dimension,

$$M_\eta \sim \mu \, \eta^{D_T-D} \qquad (2)$$

is the generalized Richardson-Mandelbrot equation, where M_η is the length of a curve (D_T=1) or the area of a surface (D_T=2) and μ is a constant measure of M_η in dimension D.

There are many methods for the experimental determination of D. With most of them, a set of measurements of a curve's length (B_η), using different yardstick lengths (η), or different resolutions, is required. An estimation of the fractal dimension (D) of the curve is given by the slope (1-D) of the Richardson-Mandelbrot plot of $\log(B_\eta)$ versus $\log(\eta)$.

A simple method consists in evaluating B_η at different microscope magnifications. The inverse of the resolution is then used instead of η (Paumgartner et al., 1981; Rigaut, 1984).

With the divider stepping method (Richardson, 1961), the boundary length is estimated by stepping along the object's contour. The results obtained by divider stepping are similar to those obtained by the magnification method (Rigaut, 1984). The divider stepping polygonation, which is not so easy to use with an automated image analyser (Rigaut, 1984, 1987ab), is nevertheless preferable to the polygonation by successive vertices spaced by equal numbers of pixels (Schwarz & Exner, 1980). Tricot *et al.* (1987) have proposed another method, based on intersecting the contour with a fitting curve.

The dilation method (Flook, 1978), based on an idea from Cantor (cf. Mandelbrot, 1982) is straightforwardly implemented in automated image analysers. The Minkowski (1901) dimension, extended by Bouligand (1928) to non-integer values, offers a sound

mathematical basis to this method. The practical application is based on successive dilations of a curve by an isotropic structuring element of diameter η , centred on successive pixels of the digitized curve. Then, $B_\eta \sim \eta^{-1} \alpha$, where α is the area of the Minkowski 'sausage' obtained by dilating the curve. Other methods, using linear structuring elements or the convex hull, have been proposed (Tricot et al., 1987).

The box method is simple to use (e.g. Feder, 1988). It can be combined with the magnification method (Morse et al., 1985). The box counting theorem (Barnsley, 1988) offers a mathematical basis to this method. The image plane containing the curve is tesselated by squares of side η , using a randomly positioned grid. The number (N_η) of squares intersected by the curve replaces the number of divider steps, and $B_\eta \sim N_\eta \eta$.

The censored intercept method (Flook, 1982) is an elegant variant of the box method. Based on the line grids used in stereology (Weibel, 1979), it consists in counting, when there are several intersections of the curve with a line segment, only those intersections which are separated by a distance larger than a given value of η . Then, $B_{\eta A} = (\pi/2)\, I_{\eta L}$, where $I_{\eta L}$ is the number of censored intersections per unit line length.

Empirical fractal laws other than equation (2) have been discovered, such as the area/perimeter (Lovejoy, 1982) and number/size (Korčak, 1938) relationships. For the former, D can be estimated by slit-island analysis (Mandelbrot et al., 1984).

Pentland (1984a) has shown that, under some assumptions of homogeneity, the two-dimensional projection of a three-dimensional Brownian fractal surface produces an image whose grey tone function is fractal.

The variogram (Matheron, 1965) may be used to estimate the dimension of a fractal Brownian function (Mandelbrot & Wallis, 1969). For such a function, the Fourier power spectrum can be used to estimate D (Mandelbrot & Van Ness, 1968).

The first works using fractal geometry in cell biology were those of Weibel's group. Weibel presented some preliminary results in 1979 (fractal dimension of 2.17 for the human lung alveolar surface). Paumgartner et al. (1981) estimated mitochondrial membrane surface area densities (S_V) stereologically in electron microscopy, at different magnifications. They concluded that mitochondrial membranes are fractal, but only up to a 'critical resolution', above which no additional structural complexity can be observed.

Fractal geometry offers a model for the analysis of the discrepancies observed between the results of stereological studies (review in Rigaut, 1987b).

Mandelbrot (1982) has proposed several fractal models for the branching of lung bronchi, for capillaries in tissues and for the surface of brain folds. A fractal model for the vascular system of the lung has been proposed (Lefèvre, 1983). The electric system of the heart might be based on an anatomically fractal conducting tissue (Goldberger et al., 1985). Fractal trajectories have been observed for the movements of spermazoa (Schoevaert-Brossault & David, 1984) and for the growth of embryonic axons (Katz, 1985; Katz & George, 1985).

The asymptotic fractal concept

The contours of most natural objects, both in biology and in materials science, do not display ideally fractal characteristics (Gelléri, 1982; Rigaut et al., 1983b; review in Rigaut, 1987b). Most object contours are ideally fractal only asymptotically, at lower resolutions (Rigaut, 1987b). At higher resolutions, the boundary length (or surface area) tends towards a maximum, and this fits real data better than by using a 'critical resolution' (Rigaut, 1984). Many authors, invoking the possible

existence of 'multifractals' (Kaye, 1978), have tried to adjust concave log-log plots with broken line segments. The subjectivity of such fittings has drawn much criticism (review in Rigaut, 1987b).

The departure of experimental results from classic fractal geometry led Rigaut (1984) to formulate the asymptotic fractal (A.F.) concept, inside which fractality is a Gestalt-like (Arnheim, 1973) 'ideal' that most object forms and textures tend to approach (Rigaut, 1986, 1987b, 1988b). The A.F. model (Rigaut, 1984) displays two asymptotic behaviours when the resolution is varied, tending towards a maximum value at high resolutions, and towards a fractal behaviour at low resolutions. The new concept allows for an asymptotic fractal dimension.

The underlying mathematics stem from an equation borrowed from enzymological biochemistry (Hill, 1910). The use of this equation in our context is empirical (this is also the case for the Richardson-Mandelbrot equation). Its choice, however, lies upon a conjecture: that cooperativity effects, which represent the basis of the interpretation of the original version of the equation in terms of kinetic behaviour of allosteric enzymes (Monod et al., 1965), are also relevant in our context. Non-linear dynamics, such as that observed in cellular automata systems (Wolfram, 1984), could represent an ontogenic explanation for the structure of natural objects. Some considerations from geostatistical theory (Rigaut, 1987b; Rigaut et al., 1987b) might also offer some indirect justifications for this equation.

The A.F. equation (Rigaut, 1984) is

$$M_\eta \sim [1 + (L^{-1}\ \eta)^{D-D_T}]^{-1}\ M_m\ , \qquad (3)$$

where M_m is the maximum value of M_η, and L ($\eta = L$ when $M_\eta = M_m/2$) are positive constants.

When $\eta \rightarrow 0$, $M_\eta \rightarrow M_m$. When $M_m \rightarrow \infty$, or when $\eta \rightarrow \infty$, then $M_\eta \rightarrow \mu\ \eta^{D_T-D}$, akin to the generalized Richardson-Mandelbrot equation (2), with $\mu = M_1 = L^{D-D_T}\ M_m$. Therefore, the A.F. model tends towards the 'ideally fractal' model when M_m and/or η become large ($\eta >> L$).

The estimation of the parameters of the A.F. equation is made by using a linearized expression (Rigaut, 1984): either $M_\eta^{-1} = (M_m\ L^{D-D_T})^{-1}\eta^{D-D_T} + M_m^{-1}$, or $\log[M_\eta^{-1}(M_m - M_\eta)] = (D-D_T)\log(\eta) - (D-D_T)\log(L)$.

The log-logistic equation, which bears a clear relationship to our A.F. equation, has been used by Gelléri (1982) to fit the concave log-log Richardson-Mandelbrot plots he observed experimentally in the study of gel pores. This equation, however, includes a minimum asymptotic value for M_η, thus differing from our A.F. equation (3) by a change of coordinates, which makes the asymptotic tendency towards an ideal fractal form at low resolutions impossible to evaluate.

Mandelbrot (in Rigaut, 1984) proposed another empirical equation, for concave log-log curves, which would bear some analogy with the Zipf-Mandelbrot law (Mandelbrot, 1953) in linguistics. However, no theoretical inference can be drawn from the use of such an equation in our context.

Underwood & Banerji (1986) have proposed another empirical equation for non-ideal fractals observed in quantitative fractography. This equation was chosen to fit reversed sigmoidal log-log curves (whose tails at lower resolutions might, in fact, be

artefactual). It does not lead to convincingly linear log-log plots, especially at high resolutions (see Fig. 4 in Banerji, 1987). Finally, its behaviour is difficult to analyse in terms of fractal theory.

The A.F. equation (Rigaut, 1984) allows remarkably precise fittings of experimental data from all sorts of objects, natural or man-made. The asymptotic fractal concept has also been used in petrophysics (Pape et al., 1987) and in metallography (Marchionni, personal communication, 1987).

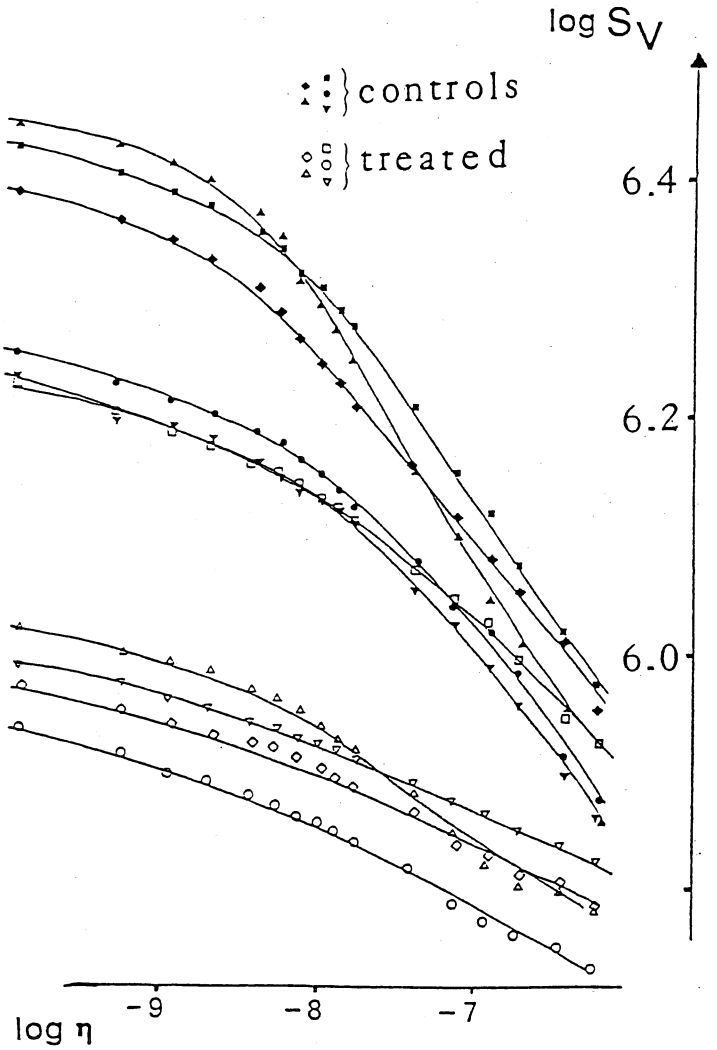

Fig. 1 (a): Richardson-Mandelbrot log-log plot for the lung alveolar S_V versus the length of the (divider stepping) yardstick representing the inverse of the resolution. Premature newborn rabbits, controls (badly inflated alveoli) or surfactant-treated (well-inflated). The asymptotic fractal tendency at low resolutions is clearly visible.

The asymptotic fractal concept has led to interesting results on the structure of lung alveoli (Rigaut, 1984, 1987b; Rigaut & Robertson, 1987; Rigaut et al., 1983b, 1987a). Neonatal rabbit lungs, badly- or well-inflated, were studied by automated image analysis (Rigaut et al., 1983a; Rigaut & Robertson, 1986), allowing the estimation of many stereological parameters, including surface area density, average integral mean curvature and inflection point-related quantities, at different resolutions. It is impossible to analyse the distribution of experimental surface area densities versus resolution by classic fractal theory, as the Richardson-Mandelbrot plots produce invariably concave curves (Fig. 1a). On the opposite, the A.F. equation fits remarkably well the data (Fig. 1b). The estimation of (asymptotic) maximum surface area densities, independent of resolution, is interesting for future applications of stereology in biology.

The L constant and the (asymptotic) fractal dimension (D) allow a (highly significant) separation between animals with badly-inflated alveoli and animals with well-inflated (surfactant-treated) alveoli. The maximum total alveolar surface area is constant, independently of whether the lungs are well-inflated or not.

The average integral mean curvature of the alveolar surface increases with the resolution, but reaches a maximum, asymptotic value. It remains constant inside a certain range of resolutions ($3.5 \leq h \leq 9$ µm), corresponding to alveolar radius values (estimated by Laplace's law) between 65 and 150 µm. These figures are in agreement with alveolar sizes, respectively for badly- and well-inflated lungs.

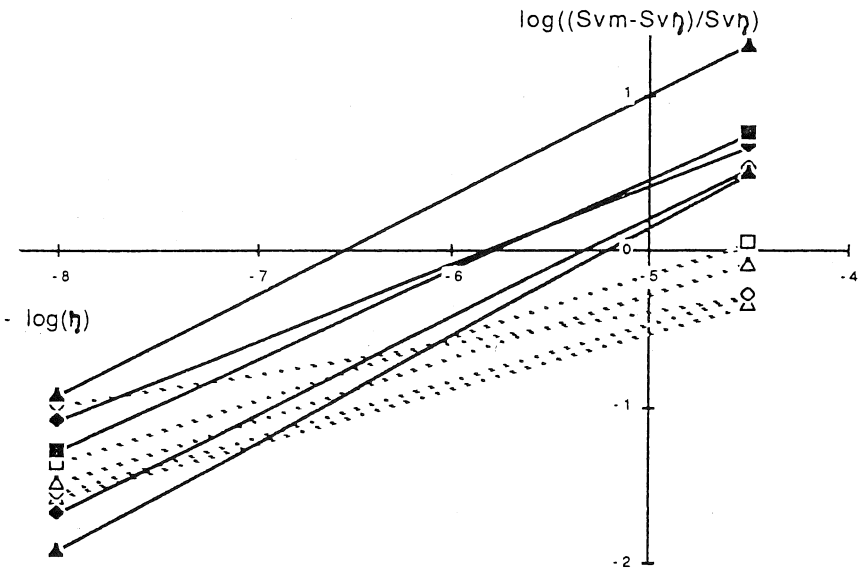

Fig. 1 (b): Hill log-log plot for the Asymptotic Fractal model, on the same data as Fig. 1(a); controls (black symbols) and surfactant-treated (white symbols); linear regression lines (all correlation coefficient are ≥ 0.99).

We have derived (Rigaut et al., 1987a) a new stereological quantity, the average integral mean curvature of saddle surface asymptotic lines ($K\sigma_S$), i.e. the integral mean curvature for saddle surface asymptotic lines ($K\sigma$) (DeHoff, 1981), averaged over the whole reference surface (S). We have shown that

$$K\sigma_{\eta S_\eta} = (\pi/2)\, I_\eta B_\eta \quad , \qquad (4)$$

where $I_\eta B_\eta$ is the density of inflection points (I) per object boundary length (B_η), for a given value of η, and $K\sigma_{\eta S_\eta}$ is the value of $K\sigma_S$ for this value of η.

Therefore, $K\sigma_{\eta S_\eta}$ can be estimated from the inflection point density of alveolar contours. The lung, which displays an A.F.-like behaviour in terms of the total alveolar curvature (cf. supra), shows an ideally fractal behaviour in terms of $K\sigma_{\eta S_\eta}$. The values of $K\sigma_{\eta S_\eta}$, at any given resolution, are the same in the animals with badly-inflated lungs and in those with well-inflated lungs (Fig. 2). Inflating the lung pushes apart the saddle surfaces without deforming them. Saddle surfaces might represent a lattice of fixed 'anchor' points, inside a self-similar fractal system (Rigaut et al., 1987a).

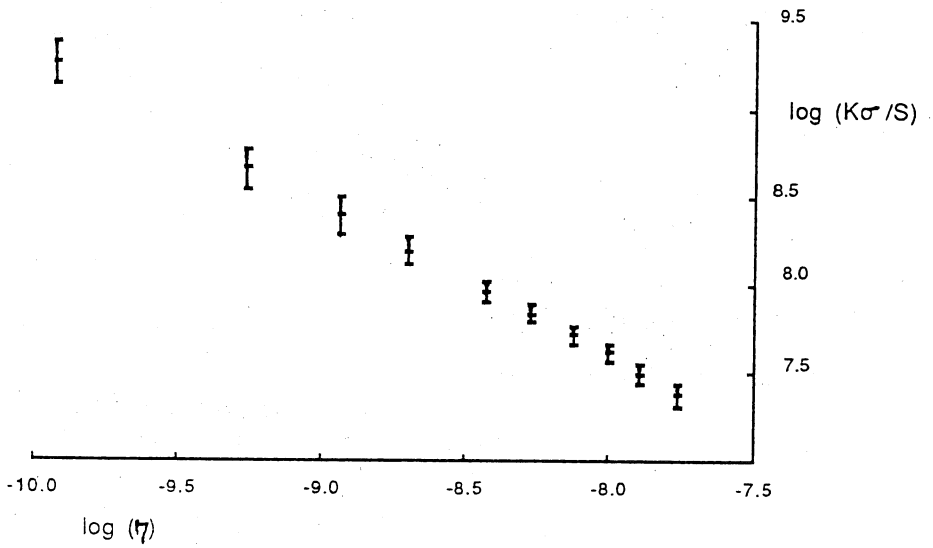

Fig. 2: Log-log plot of the average integral mean curvature of saddle surface asymptotic lines for lung alveoli, versus the divider stepping length. Means and S.Ds. for all control and treated animals (cf. Fig. 1a).

FRACTALS, MATHEMATICAL MORPHOLOGY AND VISION

Computer vision and human vision

The development of computerized image analysis is hampered by the difficulty of segmenting scenes. There is no general theory of segmentation, although some theoretical considerations may offer a rational basis for a choice among methods (Serra, 1987). Moreover, present methods for artificial vision reflect the rigidity of our concepts about computers (Frisby, 1979).

It is tempting to abandon the clumsy methodology we use at present and try to imitate human vision instead, considering its incredible efficiency and versatility. Alas, we do not know much about the mechanisms of human vision (Sutherland, 1986). Recently, however, some ideas about possible relationships between vision and fractals have started to appear.

Human vision and fractals

The fractal Brownian model allows an accurate description of the effect of changes in resolution on most homogeneous textured regions encountered in natural imagery (Medioni & Yasumoto, 1984; Pentland, 1984a). Natural textures seem to fall into a few categories only (Stevens, 1974). Our vision system might be adapted to the task of spotting efficiently such textures (Pentland, 1984ab, 1986). There is some evidence in favour of a spatial-frequency perception of texture in human vision (Richards & Polit, 1974).

The hypothesis that there are two successive steps in vision tends to replace nowadays the concept of a continuous gradient of sophistication (cf. Pentland, 1986). The first step, corresponding to a low-level scene segmentation, is generally thought to be pre-attentive. The second step would correspond to inference-based analyses, including high-level segmentation. This has been expressed by Gestalt psychologists, who have used the concept of Pragnanz to explain the pre-attentive phase of vision (Arnheim, 1973).

We are dealing with this low-level step when we consider fractal geometry as a possible framework for segmentation. The idea is based on the fact that surface textures show fractal characteristics, at least inside a certain range of resolutions. The prevalence of such surfaces may be explained by analogy with Brownian motion (Pentland, 1986). Computer-produced surfaces which look most natural are indeed fractal Brownian (e.g. Peitgen & Saupe, 1988).

Under reasonable assumptions, the projection (two-dimensional image) of a three-dimensional fractal surface is also fractal (Pentland, 1984a). Most grey tone functions from natural textured objects display fractal characteristics (Rigaut, 1988b).

Serra (1987) expressed the opinion that vision might be based on mathematical morphology-like operations. Leonardo da Vinci (cf. Kuény, 1983) had already proposed the idea that seeing is transforming. Pentland (1985) proposed a type of image transformation (based on double band-pass filterings) which seems physiologically plausible for the evaluation of the fractality of a texture by the brain.

Our works show that simple image transformations based on mathematical morphology allow an evaluation of the fractal dimension of the grey tone function in any region of an image (Rigaut, 1987a, 1988a, 1989). A combination of mathematical morphology operations with fractal geometry represents a plausible model for pre-attentive vision. Grey tone operations can indeed be understood in the context of a recursive retinal mechanism, the excitation of each successive cell being accompanied by the inhibition of surrounding cells.

Computer vision and fractals

Medioni & Yasumoto (1984) and Pentland (1984a, 1986) have expressed the idea that it might be feasible to achieve low-level image classification by evaluating the fractal dimension of the grey tone texture. Pentland (1984a) has indeed obtained some results by evaluating, in the Fourier domain, the fractal dimension of the grey tone function in different regions of an image.

Our model allows to find such regions through simple image transformations. It consists in searching for regions in which the function $\phi(x, y)$, which defines the grey tone image, can be represented, inside a certain range of resolutions, by a fractal surface. The scheme is based on the M.I.F. ('Mathematical morphology and Ideal Fractals') equation, whose derivation stems from both mathematical morphology and fractal geometry (Rigaut, 1987a, 1988a, 1989):

$$\Delta_\eta \sim K \eta^{3-D} , \qquad (5)$$

where K is a constant and

$$\Delta_\eta = V_Q\{\psi(x, y) \oplus F_\eta\} - V_Q\{\psi(x, y) \ominus F_\eta\} , \qquad (6)$$

where F_η is a disc-shaped planar structuring element (Serra, 1982), of diameter η and area $A\{F_\eta\}$, and $\psi(x, y) \oplus F_\eta$ and $\psi(x, y) \ominus F_\eta$ are the sub-graphs (Serra, 1988) which result, respectively, from the dilation and from the erosion by F_η of the sub-graph $\psi(x, y)$ of $\phi(x, y)$; $V_Q\{\cdot\}$ is the Lebesgue measure (volume) of sub-graph $\{\cdot\}$ inside a quadrat Q, of area $A\{Q\}$; the centre of F_η is inside Q and $A\{F_\eta\} << A\{Q\}$.

The M.I.F. equation allows, in log-log form, the simple computation of D from the grey level values of a series of images resulting each from the subtraction of an eroded image from a dilated one, having used a series of values of η. Quadrats of varying area must be used in the search for regions of a desired type. The search may be organized in a systematic way, but constrained iterations are preferable (Rigaut, 1988a). Our algorithm is still much too slow for routine applications.

The M.I.F. model is only valid inside specific ranges for the value of η. Grey tone surfaces are only 'ideally' fractal inside a certain range of resolutions. This has also been noted (Peleg, 1983) for Brodatz (1966) textures. Therefore, we have derived the M.A.F. ('Mathematical morphology & Asymptotic Fractals') model (Rigaut, 1990), which combines the A.F. and M.I.F. models:

$$\Delta_\eta \sim [1 + (L^{-1} \eta)^{D-D_T}]^{-1} C \eta , \qquad (7)$$

where C is a constant. This formula has two asymptotes: when $\eta \rightarrow 0$, $\Delta_\eta \rightarrow C \eta$, and, when $\eta \rightarrow \infty$, $\Delta_\eta \rightarrow L^{D-D_T} C \eta^{D_T-D+1}$.

The M.A.F. model is experimentally verified in all the natural textures we have analysed. A sufficient range of values produces the concavity of the log-log graph which is expected in the M.A.F. model, with a slope of ~ 1 for the lowest values. The position of the experimental curve is identical at different magnifications, as long as some of the smaller objects whose grey tone texture is fractal do not vanish altogether by lowering too much the resolution.

An application on a section from a newborn rabbit lung (badly inflated), at three different magnifications and using, for each of them, seven sizes for the structuring element (3 x 3 to 15 x 15 pixels), is shown in Fig. 3. The asymptotic slope for $\eta \rightarrow 0$ is equal to 1 and that for $\eta \rightarrow 0$ allows to estimate D = 2.50 . We use $\Delta_{\eta A}$ here, to render the M.A.F. equation invariant to changes in reference area (A).

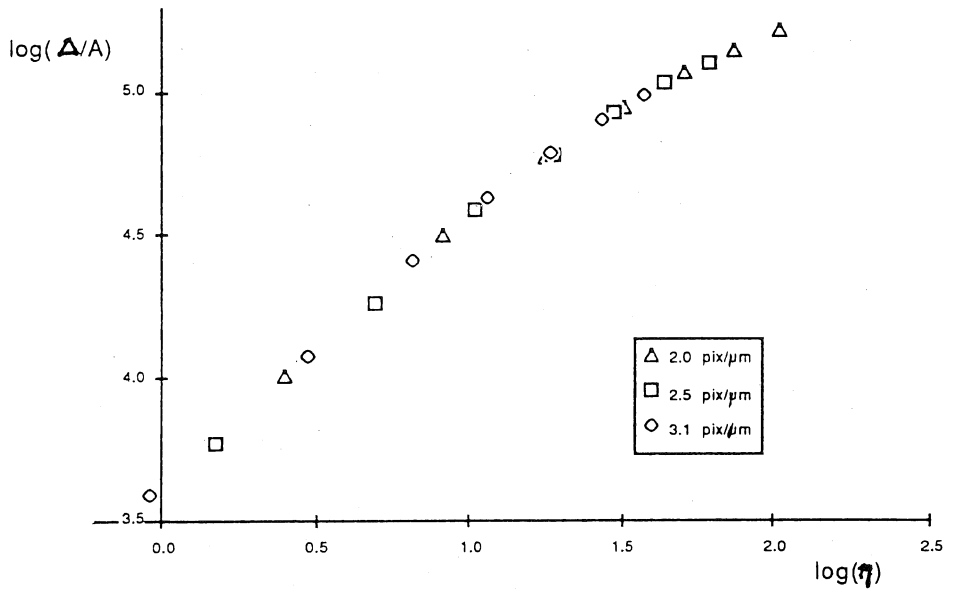

Fig. 3: Log-log plot corresponding to the M.A.F. model (cf. text).

We have experimented with our M.I.F. and M.A.F. models on numerous types of natural objects. Practically all grey tone functions we have explored yielded M.I.F.-like fractal characteristics for well-defined objects, inside specific ranges of values for η (which the M.A.F. model helps to find). Examples of object segmentation in computerized scene analyses of histological sections, from the lung and the liver, are shown in Rigaut (1987a, 1988a, 1989). Fig. 4 shows an example of the use of the M.I.F. model.

The M.I.F. model should allow some further progress in the domain of textural studies. The fractal dimension of the grey tone surface (and the other parameters derived from our model) can be used in the classification of textures (Rigaut, unpublished results

on nuclear chromatin). This represents a new development in a field which has been characterized by the quasi-exclusive use of co-occurence matrices (Haralick et al., 1973), based on Julesz's (1965) early ideas on pre-attentive texture perception through global second-order statistics.

Another possible future development is the generalization of our model to three-dimensional (3-D) images. The 3-D version of the M.I.F. equation is mathematically straightforward. We are currently studying the feasibility of segmenting, through a 3-D version of our approach, nuclei in 3-D images obtained by laser scanning confocal microscopy on thick tissues (Rigaut et al., 1988).

Serra has proposed (1988) a method for the estimation of the Minkowski (1901) dimension, also based on mathematical morphology, but using a spherical ('rolling-ball') structuring element G_η of diameter η (Sternberg, 1986). The method is based on a derivation by Minkowski (1901). With our notation (k is a constant),

$$\eta^{-1} [V_Q\{\psi(x, y) \oplus G_\eta\} - V_Q\{\psi(x, y) \ominus G_\eta\}] \rightarrow k\ \eta^{-D} , \quad \text{when} \quad \eta \rightarrow 0 . \qquad (8)$$

Rolling-ball transformations are not easy to implement in an image analyser. Moreover, Serra's method is based on the extrapolation for $\eta \rightarrow 0$, which might yield less precise results than our model (e.g. it is impossible, on a square lattice, to find an acceptably approximated spherical structuring element of width < 5 pixels); Serra (1988) suggests that, in practice, different magnifications could be used.

If a function is fractal Brownian, the following equation (Mandelbrot & Van Ness, 1968) is satisfied:

$$p(\{||\delta x||^{-H} [\phi(x)-\phi(x+\delta x)]\} < \vartheta) = F(\vartheta) , \qquad (9)$$

where $p(\cdot)$ is a probability, $F(\vartheta)$ is a cumulative distribution function and H is the Hurst exponent (cf. Mandelbrot, 1982), with $H = 1-(D-D_T)$; $\phi(x)$ and x can be interpreted as vector quantities, thus providing extension to $\phi(x, y)$.

Under the assumptions of constant illumination and albedo, and of a Lambertian surface reflectance function, the projection of a three-dimensional fractal Brownian surface onto a plane produces an image whose intensity function is fractal Brownian, with the same fractal dimension as that of the original surface (Pentland, 1984a). Therefore, if the original surface corresponds to a real relief, its fractal dimension can be estimated by using our M.I.F. model on a photograph.

CONCLUSION

Pentland (1986) states that "A theory of visual function that has no model of the world also has no meaning" and that "Theories of visual function, therefore, are based on models (...) of how the world is structured and of how this structure is evidenced by regularities in the image". Heisenberg (1970) suggested that "The structures of our minds may perhaps reflect the world's internal structure". We believe that there is a strong coherence in a work based on studying first the real world through fractal models, and then turning to the problem of human vision.

a

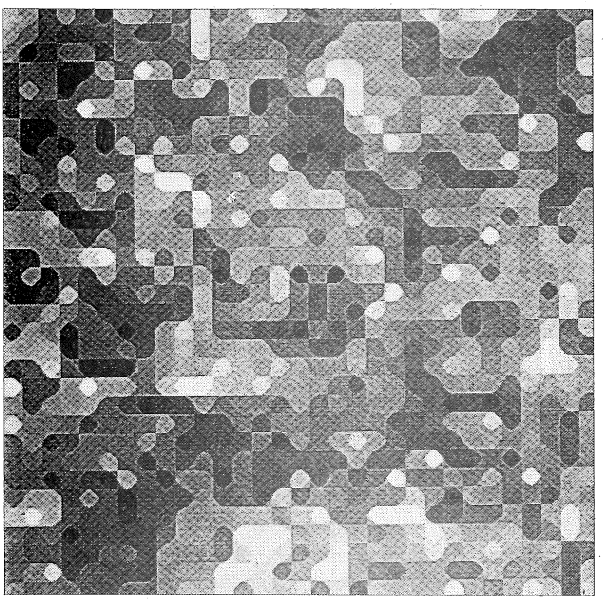

b

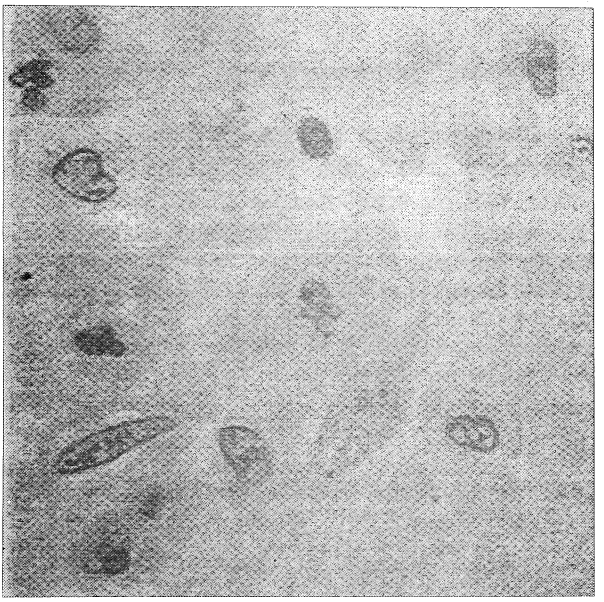

Fig. 4: Calibration: 7.6 pixels/μm; (a): Original digitized image; Feulgen-stained section from an oesophagus cancer; (b): 'image of D', hypo-median filtered (9x9, rank 45); D is evaluated by the M.I.F. model in systematic quadrats (8x8) and coded into grey levels (0-255).

c

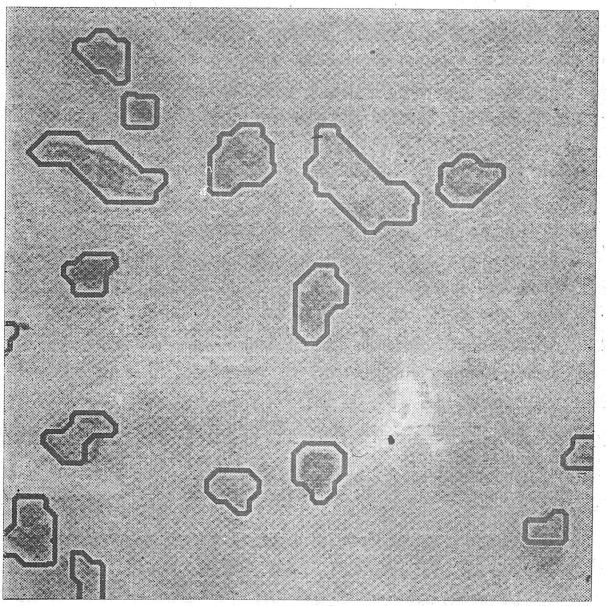

d

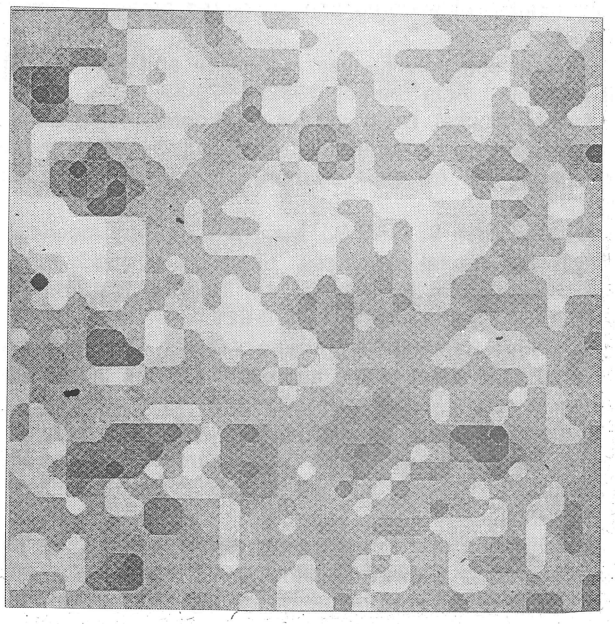

Fig. 4: (c): 'Image of K', hypo-median filtered (15x15, rank 113) and contrast-inverted; K (cf. equation 5) is evaluated in parallel with D (cf. Fig. 4b) and coded into grey levels (0-255); (d): Segmentation of nuclei, obtained by a combination of optimal values for D (2.05 to 2.33) and Ψ, and binary closings.

ACKNOWLEDGEMENTS

The author is grateful to Dr. Bengt Robertson and to Mrs. Paulette Herlin for the histological slides used, respectively, for Figs. 1-3 and for Fig. 4, to Dr. Angela M. Downs for her help in preparing the Figures and to the Association pour la Recherche sur le Cancer and the Université Paris 7 for grants.

REFERENCES

Arnheim R. La Pensée Visuelle. Paris: Flammarion, 1973.

Banerji K. Estimation of the "true" fracture roughness parameters by iterative optimization of a reversed sigmoidal fractal model. Acta Stereol. 1987; 6/3: 815-820.

Barnsley M. Fractals Everywhere. San Diego: Acad. Press, 1988.

Bouligand G. Ensembles impropres et nombre dimensionnel. Bull. Sci. Math. 1928; 2/52: 320-334 & 361-376.

Brodatz P. Textures: A Photographic Album for Artists and Designers. New York: Dover, 1966.

DeHoff RT. Stereological meaning of the inflection point count. J. Microsc. 1981; 121: 13-19.

Falconer KJ. The Geometry of Fractal sets. Cambridge: Cambridge Univ. Press, 1985.

Feder J. Fractals. New York: Plenum Press, 1988.

Flook AG. The use of dilation logic on the Quantimet to achieve fractal dimension characterization of textured and structured profiles. Powder Technol. 1978; 21: 295-298.

Flook AG. Fractal dimensions: their evaluation and their significance in stereological measurements. Acta Stereol. 1982; 1: 79-87.

Frisby JP. Seeing, Illusion, Brain and Mind. Oxford: Oxford Univ. Press, 1979.

Gelléri B. Bestimmung der Porenradienverteilung der Trägermatrix Eupergit C und ihre Beschreibung als fraktales System. Thesis, Gießen: Justus-Liebig-Universität, 1982.

Goldberger AL, Bhargava V, West BJ, Mandell AJ. On a mechanism of cardiac electrical stability - The fractal hypothesis. Biophys. J. 1985; 48: 525-528.

Haralick RM, Shanmugam K, Dinstein J. Textural features for image classification. I.E.E.E. Trans. S.M.C. 1973; 3: 610-621.

Heisenberg W. Natural Law and the Structure of Matter. London: Rebel Press, 1970.

Hill AV. The possible efect of the aggregation of the molecules of hemoglobin on its dissociation curves. J. Physiol. (London) 1910; 40: 4-7.

Julesz B. Texture and visual perception. Sci. Am. 1965; 212: 38-48.

Katz MJ. How straight do axons grow ? J. Neurosci. 1985; 5: 589-595.

Katz MJ, George EB. Fractals and the analysis of growth paths. Bull. Math. Biol. 1985; 47: 273-286.

Kaye BH. Specification of the ruggedness and/or texture of a fine particle profile by its fractal dimension. Powder Technol. 1978; 21: 1-16.

Kohonen T. An introduction to neural computing. Neural Networks 1988; 1: 3-16.

Korč ak J. Deux types fondamentaux de distribution statistique. Bull. Inst. Intern. Stat. 1938; 3: 295-299.

Kuény P. Les métamorphoses des signes et connaissance de soi. Thèse de Doctorat de Spécialité (Arts Plastiques), Univ. Paris I, 1983, n°810500H.

Lefèvre J. Teleonomical optimization of a fractal model of the pulmonary arterial bed. J. Theor. Biol. 1983; 102: 225-248.

Lovejoy S. Area-perimeter relation for rain and cloud areas. Science 1982; 216: 185-187.

Mandelbrot B. Contribution à la théorie mathématique des communications. Thèse Doct. ès Sci. Maths., Publ. Inst. Stat. Univ. Paris, Ser. A, vol. 2, n°2521, 1953.

Mandelbrot BB. How long is the coast of Britain? Statistical self-similarity and fractional dimension. Science 1967; 156: 636-638.

Mandelbrot BB. The Fractal Geometry of Nature. San Francisco: Freeman, 1982.

Mandelbrot BB, Passoja DE, Paullay AJ. Fractal character of fracture surfaces of metals. Nature 1984, 308: 721-722.

Mandelbrot BB, Van Ness JW. Fractional Brownian motions, fractional noises and applications. S.I.A.M. Rev. 1968; 10: 422-437.

Mandelbrot BB, Wallis JR. Computer experiments with fractional Gaussian noises. Water Res. Res. 1969; 5: 228-267.

Matheron G. Les Variables Régionalisées et leur Estimation. Paris: Masson, 1965.

Medioni G, Yasumoto Y. A note on using the fractal dimension for segmentation. Annapolis: I.E.E.E. Computer Vision Workshop, 1984.

Minkowski H. Über die Begriffe Länge, Oberfläche und Volumen. Jahresb. Dtsch. Math. 1901; 9: 115-121.

Monod J, Wyman J, Changeux JP. On the nature of allosteric transitions. A plausible model. J. Mol. Biol. 1965; 12: 88-118.

Morse DR, Lawton JH, Dodson MM, Williamson MH. Fractal dimension of vegetation and the distribution of arthropod body lengths. Nature 1985; 314: 731-733.

Pape H, Riepe L, Schopper JR. Theory of self-similar network structures in sedimentary and igneous rocks and their investigation with microscopical and physical methods. J. Microsc. 1987; 148: 121-147.

Paumgartner D, Losa G, Weibel ER. Resolution effect on the stereological estimation of surface and volume and its interpretation in terms of fractal dimensions. J. Microsc. 1981; 121: 51-63.

Peitgen HO, Saupe D. (eds.) The Science of Fractal Images. New York: Springer-Verlag, 1988.

Peleg S. Internal Report n°TR-1306. College Park: Univ. Maryland, Dept. Comput. Sci., 1983.

Pentland AP. Fractal-based description of natural scenes. I.E.E.E. Trans. P.A.M.I. 1984a; 6: 661-674.

Pentland AP. Perception of three-dimensional textures. Invest. Ophtalmol. & Visu. Sci. 1984b; 25: 201.

Pentland AP. On describing complex surface shapes. Image & Vision Comput. 1985; 3: 153-162.

Pentland AP. Perceptual organization and the representation of natural form. Artif. Intell. 1986; 28: 293-331.

Richards W, Polit A. Texture matching. Kybernetik 1974; 16: 155-162.

Richardson LF. The problem of contiguity: an appendix to statistics of deadly quarrels. Gen. Syst. Yearb. 1961; 6: 139-187.

Rigaut JP. An empirical formulation relating boundary lengths to resolution in specimens showing "non-ideally fractal" dimensions. J. Microsc. 1984; 133: 41-54.

Rigaut JP. Fractalité et modélisation en biologie. In: Synergie et Cohérence dans les Systèmes Biologiques - 1985, Wolkowski Z (ed.). Paris: Université Paris 7, 1986, pp. 83-91.

Rigaut JP. Natural objects show fractal grey tone functions - a novel approach to automated image segmentation, using mathematical morphology. Acta Stereol. 1987a; 6/3: 799-802.

Rigaut JP. Fractals, semi-fractals et biométrie. In: Fractals - Dimensions Non Entières et Applications, Cherbit G (ed.). Paris: Masson, 1987b, pp. 231-281.

Rigaut JP. Automated image segmentation by mathematical morphology and fractal geometry. J. Microsc. 1988a; 150: 21-30.

Rigaut JP. Analyse d'images: reconnaissance de forme, ou de structure ? Quelques idées pour une réflexion théorique. In: Biologie Théorique - Solignac 1986, Kretzschmar A (ed.). Paris: Eds. CNRS, 1988b, pp. 141-160.

Rigaut JP. Automated image segmentation by fractal grey tone functions. Gegenb. Morphol. Jahrb. Leipzig 1989; 135: 77-82.

Rigaut JP. Fractals in biological image analysis and vision. In: Fractal objects, Losa G (ed.). Locarno: Ist. Matem. Tessino, 1990, in press.

Rigaut JP, Berggren P, Robertson B. Automated techniques for the study of lung alveolar stereological parameters with the IBAS image analyser on optical microscopy sections. J. Microsc. 1983a; 130: 53-61.

Rigaut JP, Berggren P, Robertson B. Resolution-dependence of stereological estimations: interpretation, with a new fractal concept, of automated image analyser-obtained results on lung sections. Acta Stereol. 1983b; 2/S1: 121-124.

Rigaut JP, Berggren P. Robertson B. Stereology, fractals and semi-fractals - the lung alveolar structure studied through a new model. Acta Stereol. 1987a; 6/1: 63-67.

Rigaut JP, Lantuéjoul C, Deverly F. Relationship between variance of area density and quadrat area - interpretation by fractal and random models. Acta Stereol. 1987b; 6/1: 107-113.

Rigaut JP, Robertson B. Quantitative evaluation of neonatal lung expansion with automated image analysis. Ped. Pathol. 1986; 6: 11-24.

Rigaut JP, Robertson B. Modèles fractals en biologie. J. Microsc. Spectrosc. Electron. 1987; 12: 163-168.

Rigaut JP, Vassy J, Carvajal S, Downs AM, Nguyen Q, El Kebir FZ, Foucrier J. Three-dimensional histo-morphometry by laser scanning confocal microscopy. Cytometry 1988; S2: 86, Abstr. n°567D.

Schoevaert-Brossault D, David G. Approche fractale de l'analyse de la forme des trajectoires des spermatozoïdes humains. Biol. Cell 1984; 52: 126a.

Schwarz H, Exner HE. The implementation of the concept of fractal dimension on a semi-automatic image analyser. Powder Technol. 1980; 27: 207-213.

Serra J. Image Analysis and Mathematical Morphology. London: Acad. Press, 1982, Vol.1.

Serra J. Morphological optics. J. Microsc. 1987; 145: 1-22.

Serra J. Image Analysis and Mathematical Morphology. London: Acad. Press, 1988, Vol.2.

Sternberg SR. Grayscale morphology. Comput. Vision Graph. & Image Process. 1986; 35: 333-355.

Stevens S. Patterns in Nature. Boston: Atlantic-Little, 1974, Brown Books.

Sutherland S. How does the brain do it ? Nature 1986; 322: 415.

Tricot C, Wehbi D, Quiniou JF, Roques-Carmes C. Concepts of non-integer dimension applied to image treatment. Acta Stereol. 1987; 6/3: 839-844.

Underwood EE, Banerji K. Fractals in fractography. Mater. Sci. Engin. 1986; 80: 1-14.

Weibel ER. Stereological Methods. Practical Methods for Biological Morphometry. London: Acad. Press, 1979, Vol. 1.

Wolfram S. Cellular automata as models of complexity. Nature 1984; 311: 419-424.